Journal of Sol-Gel Science and Technology (2019) 89:521–530
https://doi.org/10.1007/s10971-018-4888-3

ORIGINAL PAPER: SOL-GEL AND HYBRID MATERIALS FOR BIOLOGICAL AND HEALTH (MEDICAL) APPLICATIONS

In vitro drug release study from hydroxyapatite-alumina composites

J. M. C. Teixeira[1,2] · J. S. V. Alburquerque[1] · E. B. Duarte[1] · S. A. Silva[1] · R. E. F. Q. Nogueira[1]

Received: 10 August 2018 / Accepted: 17 November 2018 / Published online: 29 November 2018

Abstract

Modern technologies require new materials with an increasingly varied set of properties. In this context, biomaterials such as synthetic hydroxyapatite have become of great interest for research and development in the field of materials science and engineering. In spite of its biocompatibility, hydroxyapatite suffers from low mechanical strength. Aiming to improve the mechanical properties of hydroxyapatite without affecting its biocompatibility, the formation of hydroxyapatite composites with alumina (Al_2O_3) as a reinforcement has been studied. In this work, hydroxyapatite was synthesized via a sol–gel method. Hydroxyapatite/alumina composites (HAp/Al_2O_3) were prepared in different proportions to determine the best combination to be used as a controlled release system of ampicillin. The samples obtained were characterized by X-ray diffraction and scanning electron microscopy. Mechanical behavior was evaluated by diametrical compression. After characterization of the composites, the sample with the highest mechanical resistance was chosen for the incorporation and release of ampicillin. The study showed very different release profiles, indicating that the release devices prepared may be useful in clinical applications that require varying times for treatment.

Graphical Abstract

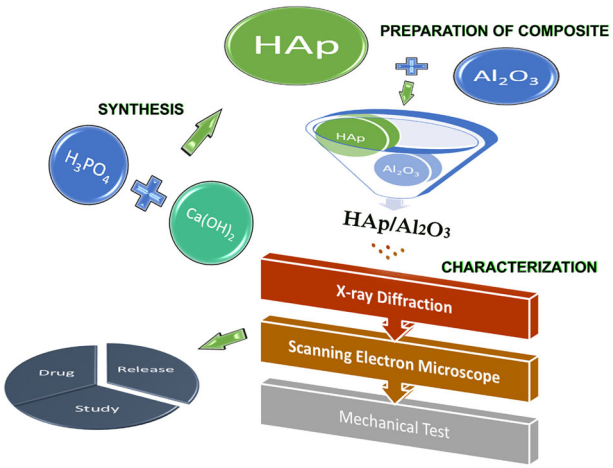

✉ J. M. C. Teixeira
joelanecarvalhot@hotmail.com

[1] Biomaterials Laboratory, Department of Metallurgical and Materials Engineering, Federal University of Ceará, Fortaleza, CE, Brazil

[2] Federal Institute of Education, Science and Technology of Sertão Pernambucano, Ouricuri, PE, Brazil

Highlights

- Hydroxyapatite successfully synthesized by the sol–gel method.
- Formation of hydroxyapatite composites with alumina as a reinforcement has been studied.
- Addition of alumina increased mechanical strength of the hydroxyapatite.
- A composite with the highest mechanical resistance was chosen for release of ampicillin.
- Release study revealed great potential of the composites for use in ampicillin delivery systems.

Keywords Hydroxyapatite · Sol–gel · Alumina · Composites · Drug release.

1 Introduction

The last few decades have witnessed rapid growth in the search for new drug delivery systems [1, 2] and the study of porous biomaterials has opened up new possibilities for applications to nanoscience, especially in development of systems that allow incorporation and release of pharmaceutical molecules. This is because these substances have some characteristics that are essential for the physiological and therapeutic applications like structure, arrangement of ordered pores, and narrow pore distribution. In this context, natural and synthetic materials, including calcium phosphates, inorganic silica, as well as organic polymers have been studied as substrates for transporting therapeutic agents [3–5].

Drug delivery systems can maintain the concentration of the drug below the limit of toxicity, which improves the therapeutic efficacy and reduces the toxicity and the side effects, bringing more comfort to the patient. In addition, they should be able to deliver the bioactive agent precisely at the target site at a specific rate. The use of these systems reduces dosing frequency [6].

Hydroxyapatite has been widely used as an effective matrix for the encapsulation and controlled release of biologically active drugs, proteins, and other molecules. The hydroxyapatite (HAp), represented by the chemical formula of $Ca_{10}(PO_4)_6(OH)_2$ with Ca/P of ratio 1.67 [7–9], presents a series of biologically interesting properties, such as similarity to bone tissue, stable porous structures, biocompatibility, osteoconductivity, and noninflammatory character [10]. Besides that, HAp stoichiometry has great significance, since slight imbalances in the Ca/P ratio may lead to the formation of other phases that affect the interaction of the material with biological tissues. The synthesis of HAp has been performed by several methods, involving precipitations in aqueous solutions, solid-state reactions, hydrothermal methods, and sol–gel process [11]. It is worth noting that the sol–gel process has attracted researchers' attention because it allows mixing of calcium and phosphorus precursors at the molecular level [12], leading to formation of high-purity HAp at low processing temperatures.

Modern technologies require new materials with a varied set of properties. In order to improve the mechanical properties of hydroxyapatite without affecting its biocompatibility, some studies have evaluated the formation of hydroxyapatite composites added to alumina (Al_2O_3). Earlier reported work [13] suggested the possibility to incorporate Al_2O_3 with hydroxyapatite to enhance the mechanical properties but not to degrade the biocompatibility. In fact, among some reinforced materials, Al_2O_3 loaded with HAp shows better mechanical stability and biocompatibility [14]; alumina has no harmful effect on cells and tissues [14–16]. Because Al_2O_3 is a bioinert material that presents high resistance to the mechanical tensions [16], it is the one of the most widely investigated reinforcement materials for HAp bioceramics [17].

In this work, hydroxyapatite powders (molar ratio of Ca/P = 1.67) were synthesized by sol–gel process and hydroxyapatite/alumina (HAp/Al_2O_3) composites were prepared in the concentrations of 5, 15, and 30 wt% of alumina to be used as systems of incorporation and release of drugs. The characterization studies were performed using the following techniques: X-ray diffractometry for the identification of amorphous and crystalline phases, scanning electron microscopy for the observation of the morphology of the samples, and diametral compression for the evaluation of the mechanical resistance. Composites prepared with hydroxyapatite and 15 wt% of alumina were chosen for the ampicillin release study because of the similar resistance to spongy bone tissue. Ampicillin was chosen because it is one of the most common antibiotics used in the treatment of a number of bacterial infections. However, its oral administration can cause side effects such as diarrhea, nausea, depression, fatigue, ischemic colitis, thrombosis, and others. For certain treatments, such as hypertension, the development of controlled release devices can minimize this type of discomfort for the patient, since the concentration of the drug tends to remain at a controllable level in the blood stream for a longer period.

2 Materials and methods

2.1 Synthesis and sintering

Hydroxyapatite powder was synthesized by the sol–gel method. Calcium hydroxide [$Ca(OH)_2$] 0.5 M and

phosphoric acid (H_3PO_4) 0.3 M were used as starting materials for the synthesis (Eq. 1).

$$10Ca(OH)_2+6H_3PO_4 \rightarrow Ca_{10}(PO_4)_6(OH)_2+18H_2O \quad (1)$$

The addition of phosphoric acid was controlled to achieve approximately constant flow rate of 8 ml/min and the resultant solution was kept under constant stirring at room temperature for 1 h. The suspensions were aged for 24 h. At the end of the aging period, the solution was heat-treated for gel formation. The gel was oven-dried at 80 °C for 24 h. Finally, the material was deagglomerated using an agate mortar and submitted to thermal treatment to improve crystallinity and to promote densification. The sintering process was done in a muffle furnace at 1200 °C for 2 h at a heating rate of 10 °C/min.

2.2 Characterization

The sintered material was characterized by X-ray diffraction (XRD) and scanning electron microscopy (SEM). X-ray diffraction analyses were performed on an X-ray diffractometer (XPERT Pro MPD), using CoKα radiation. The diffraction data were collected in the 2θ range from 20° to 60° at a voltage of 40 kV and a current of 40mÅ. The crystalline species were identified using the X'Pert HighScore Plus and comparison of the XRD pattern of each sample on the database JCPDS (Joint Committee Power Diffraction Standards).

The crystallinity index (CI) is a measure of the percentage of crystalline material in a given sample and it is also correlated to the degree of order within the crystals [9]. Hydroxyapatite crystalline index was calculated using the Landi et al. [18] method.

Nitrogen sorption measurements were performed on the Autosorb–Quantachrome NOVA 1200 which consists of an automated physical adsorption system that provides adsorption and desorption equilibrium data. The adsorbed and desorbed volume data at various relative pressures were used to generate information on surface area, pore volume, distribution, and average pore size.

The surface morphology of the samples was analyzed by SEM on a Quanta 450FEG-FEI scanning electron microscope. Prior to SEM analysis, the samples were fixed in a support using double-sided carbon tape and subsequently covered with a thin layer of carbon using Bal-Tec vacuum deposition system. The average diameters of the pores were determined using the ImageJ program (National Institute of Health—NIH).

2.3 Production of composites (HAp/Al_2O_3)

Composites were prepared with hydroxyapatite and 5, 15, and 30 wt% of alumina. The biphasic compositions were blended in a high-energy attrition *mill*, NETZSCH, with zirconium spheres at 350 rpm during 30 min. This method allowed obtaining a better dispersion of phases during the blending process. Subsequently, green specimens with dimensions of 12 mm in diameter and 6 mm in height were produced by uniaxial pressing using a load of 2 ton in a 15-ton (Universal) press. After demolding, the specimens were sintered in a muffle furnace at a temperature of 1200 °C for 2 h at a heating rate of 10 °C/min. At the end of the process, the composites were characterized by XRD, SEM, and diametral compression mechanical strength to select the composite with the best properties to study in vitro release.

2.4 Statistical analysis

Statistical analyses of mechanical properties were performed using ANOVA (single factor variance analysis) to verify if the arithmetic means between the treatments were statistically significant and Tukey–Kramer Multiple Comparison procedure to determine which pairs of means have statistically significant differences [19]. For statistical data, the Origin® 8 program was used.

2.5 Ampicillin in vitro release assay

The composite with higher mechanical strength was chosen for the incorporation of ampicillin. The sample was trapped in a platinum wire and submerged in a beaker containing 100 ml of phosphate-buffered saline (PBS) (pH 7.4) at a constant stirring rate of 50 rpm and temperature of 37 °C. One milliliter aliquots were withdrawn at certain time periods, replenished with buffer solution, and diluted to 2 ml with PBS. Absorbance was measured using a quartz cuvette and a wavelength of 215 nm on a Thermo Scientific Biomate 3 UV-Visible Spectrophotometer to estimate the amount of ampicillin released. The results were expressed as the percentage of released drug as a function of time.

2.6 Mathematical models

In the present work, two different dissolution models were applied to drug release data in order to evaluate release mechanisms and kinetics. The criteria for selecting the most appropriate model was based on linearity (coefficient of correlation). The mathematical models used to describe the drug release were Higuchi [20] and Korsmeyer–Peppas [21]. Experimentally, the release kinetics can be described by the Higuchi equation (Eq. 2). In this case, the quantity released versus the square root of time ($t^{1/2}$) presents linear behavior for systems based on the diffusion mechanism.

$$M_t = k\, t^{1/2} \quad (2)$$

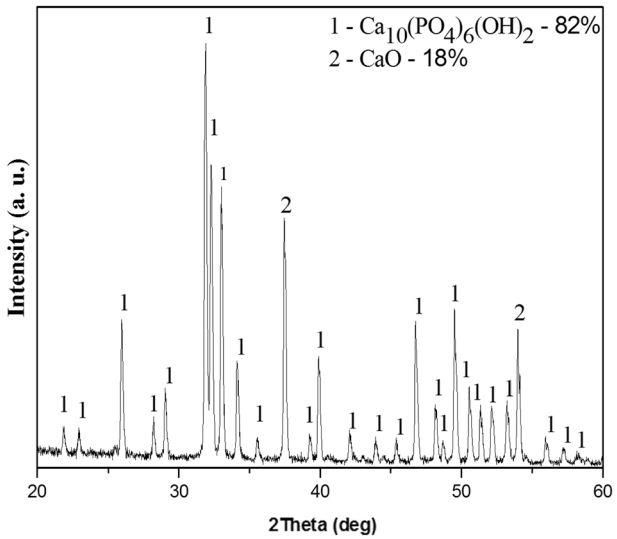

Fig. 1 XRD patterns of precursor powder sintered at 1200 °C for 2 h

where M_t is the total amount of drug released, k is the release constant, and t is time.

Eq. 3 represents the Korsmeyer–Peppas model:

$$M_t/M_\infty = K\,t^n \tag{3}$$

where M_t and M_∞ are the cumulative masses of the drug released at a time t and an infinite time, respectively. K is the proportionality constant and n is the release exponent. According to the numerical value n, the mechanism of drug release is described. If $n > 0.5$, non-Fickian diffusion is observed [22].

3 Results and discussion

3.1 Characterization of powder synthesized via sol–gel

Figure 1 shows XRD patterns from the precursor powder after sintering at 1200 °C for 2 h. Hydroxyapatite was identified as a priority phase, $Ca_{10}(PO_4)_6(OH)_2$, JCPDS: 009-0432. There is a minor phase present in the compound corresponding to calcium oxide (CaO), JCPDS: 075-0264.

Some reports on the sol–gel-derived HAp indicate that synthesis of HAp is always accompanied by the secondary phase of calcium oxide [23]. According to Best et al. [24], slight imbalances of the stoichiometric composition may contribute to the decomposition of hydroxyapatite during sintering processes and formation of new phases such as CaO.

Santos et al. [25] observed formation of CaO, similar to the data from this article. They prepared HAp via aqueous precipitation reaction by three synthetic routes. Route 1 (R1) was represented by Eq. 1. According to the authors, the aqueous process for the preparation of HAp based on R1 provided a reaction where anions of the phosphate solution (PO_4^{-3}) precipitated slowly in calcium metal ions (Ca^{+2}) suspension. The acid was dropped into alkaline suspension so that the hydroxyl ions present in $Ca(OH)_2$ suspension were exhausted by H_3PO_4 solution. However, an extra amount of calcium stayed in the precipitated HAp, forming a new phase calcium oxide (CaO), besides the hydroxyapatite. Manoj et al. [26] using $Ca(OH)_2$ and H_3PO_4 as a starting precursor, noted that the HAp was formed alongside CaO. They suggested that this may have been due to the exhaustion of hydroxyl ions present in the $Ca(OH)_2$ solution by H_3PO_4.

Table 1 Notations adopted to identify the prepared specimens

Specimen	Alumina (%m/m)	Notation
Hydroxyapatite	0	HAp-00
Hydroxyapatite	5	HAp-05
Hydroxyapatite	15	HAp-15
Hydroxyapatite	30	HAp-30
Hydroxyapatite with drug	15	HApF-15

3.2 Characterization of composites

In order to facilitate the analysis of the results, formulations were named as follows (Table 1):

The XRD patterns of HAp-05, HAp-15, and HAp-30 are presented in Fig. 2a–c with quantitative analysis of the present phases.

The absence of alumina peaks in the XRD pattern indicates that alumina reacts with HAp and forms another phase. A similar observation was made by Juang and Hon [13] and Viswanath and Ravishankar [17].

The results indicate the presence of hydroxyapatite, JCPDS: 009-0432; β-tricalcium phosphate (β-TCP), JCPDS: 070-2065; and calcium aluminate ($CaAl_2O_4$), JCPDS: 070-0134.

The analysis of the diffractograms suggests that the higher the amount of alumina added, the greater the amount of aluminate formed. In a previous study, Viswanath and Ravishankar [17] noted that most of the aluminates that are formed are alumina-rich. Apparently, the addition of alumina also reduces the crystallinity of hydroxyapatite. The crystallinity calculated for HAp-00 was 93.77%, whereas for HAp-30 it was 84.92%.

The reduction of the amount of hydroxyapatite derives from this formation of $CaAl_2O_4$ and from the thermal decomposition of HAp in β-TCP [11]. These results are in agreement with the literature. The presence of alumina in the hydroxyapatite matrix can modify the surface diffusion

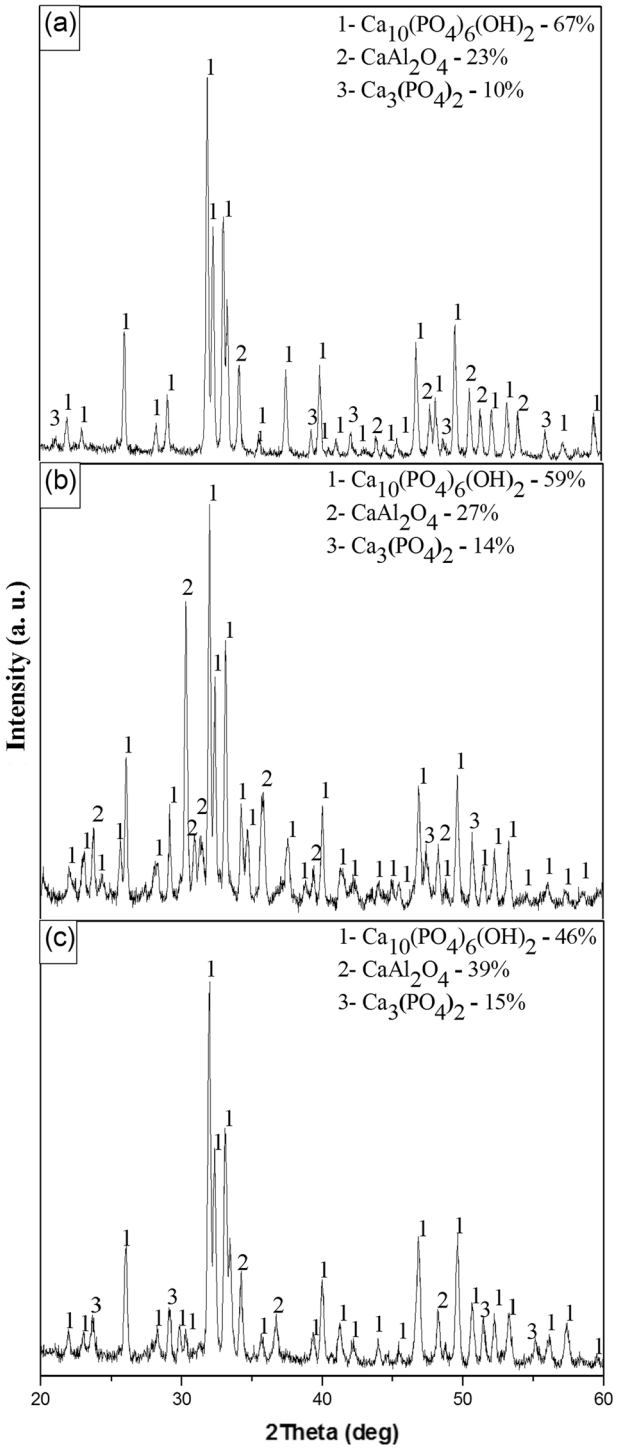

Fig. 2 XRD patterns of **a** HAp-05, **b** HAp-15, and **c** HAp-30

kinetics of HAp, leading to its decomposition into β-TCP (or α-TCP) and the subsequent formation of calcium aluminate phases. In earlier studies [13, 27], third phases such as $Ca_3Al_2O_6$ and $CaAl_2O_4$ were observed at higher temperatures (1200–1400 °C) in composites of HAp/Al_2O_3. It was concluded that HAp decomposed into CaO and $Ca_3(PO_4)_2$ and then reacted with alumina to form calcium aluminates. Usually, HAp decomposes into β-TCP around 1200 °C [17].

Phase changes of composite biomaterials in the solid state occur by the diffusion of the ions through the grain boundaries [17]. For example, the diffusion of the Al^{3+} ions occurs at the interface of the alumina grains. Ca^{2+} ions come from the calcium oxide resulting from the decomposition of HAp into β-TCP [17, 28, 29].

Table 2 Results of sorption measurements

Specimen	S_{BET} (m^2/g)	D_p (nm)	Vp (cm^3/g)
HAp-05	16.33	8.80	0.04
HAp-15	31.82	3.00	0.02
HAp-30	16.32	6.53	0.03

S_{BET} specific surface area, D_p average pore diameter, V_p total pore volume

3.3 Sorption measurements

Table 2 shows the results obtained from N_2 adsorption measurements showing differences in the specific surface area (S_{BET}), pore diameter (D_p), and pore volume (V_p). The observed pore diameter decreased from 8.8 to 3.00 nm when the amount of alumina increased from 5 to 15% and had an increase in the composite with 30% of alumina concentration. Surface areas were also measured. An increase to 31.82 m^2/g was observed for the HAp-15, with a decrease to 16.32 m^2/g in the HAp-30. It also can be noted that the pore diameter of HAp-15 is lower than that of the other formulations.

The pore size distribution graphs are show in Fig. 3. A very narrow pore size distribution, centered on a pore diameter value, is a typical characteristic of mesoporous materials with a well-ordered structural arrangement. This feature makes the synthesized materials very important for application as a device for controlled release of drugs, since the behavior is influenced by the kinetics of release through the pores of the matrices.

3.4 Morphological characterization

Microstructure development during sintering (1200 °C) was studied by SEM (Fig. 4a–d). Figure 4a shows an irregular grain growth, a heterogeneous microstructure, and the presence of inter- and intragranular pores (of around 603 nm according to the image analysis). Sintering process was confirmed by formation of intergranular contacts, intergrain's neck formation, and grain growth. These results are similar to those obtained by other authors [18, 30].

High dispersion of alumina and densification was achieved at HAp-05 and HAp-15 compositions (Fig. 4b, c). Generally, the mechanical properties increase when the

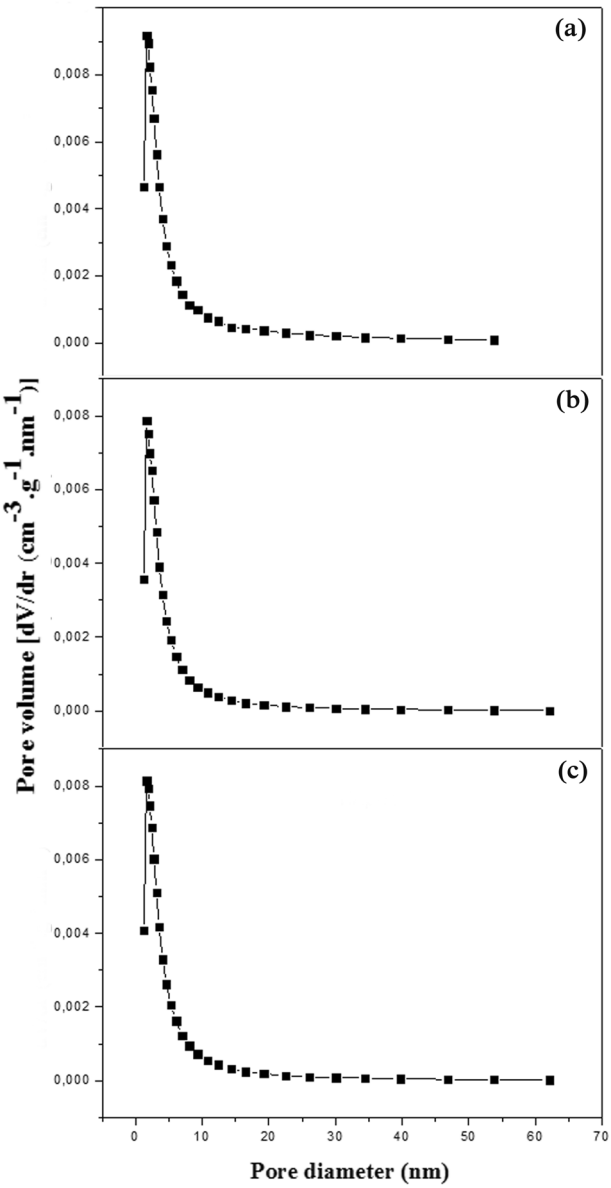

Fig. 3 Pore size distribution of **a** HAp-05, **b** HAp-15, and **c** HAp-30

density is increased [31]. Mezahi et al. [31] studied the ability to form bone-like apatite on the surface of both pure natural hydroxapatite (N-HAp) and natural hydroxyapatite containing 5 wt% of ZrO_2 or TiO_2 or Al_2O_3, sintered at 1300 °C for 2 h. It has been noticed that ZrO_2 additions did not affect the density of N-HAp samples. In the case of TiO_2, partial decomposition was accompanied with a decrease in density. Finally, for HAp–Al_2O_3, the specimens were highly densified. In agreement with the referenced work, we believe that in our study, alumina played a fundamental role in the densification process.

According to the literature, the densification of a crystalline powder can be influenced by the presence of a second phase (either in an intergranular and intragranular position) in the ceramic matrix, especially when the compaction process of such heterogeneous ceramics precedes the sintering. This phenomenon can lead to the destabilization of the interfaces, due to the presence of interfacial diffusion, and cause the modification of the crystalline structures and transformation of new phases [27, 32]. Therefore, a second phase of alumina in an intergranular and intragranular position within the hydroxyapatite matrix can directly influence the composite's sinterability and strongly alter the hydroxyapatite decomposition, leading to the formation of calcium aluminate precipitates at the grain boundaries in the HAp matrix, as already observed [17, 28]. In this sense, scanning electron microscopy characterization showed modification of the microstructures of HAp-05, HAp-15, and HAp-30 when compared to HAp-00. Moreover, the presence of aluminate ($CaAl_2O_4$) was confirmed by X-ray diffraction.

3.5 Mechanical resistance

According to Bartonickova et al. [33], alumina is a cost-effective and well-accessible option for enhancing HAp properties, especially the mechanical properties. In the present study, diametral compression resistance calculated for HAp was about 1.7 MPa. The measured values for HAp–Al_2O_3 composites are in the range of 3.7–8.4 MPa. The diametral compression resistance data for all the treatments studied are listed in Table 3.

Figure 5 shows compressive strength versus alumina fraction incorporated into the hydroxyapatite. It is noted that an increase in the additive content generates an initial increase in strength until the limit of about 15%. Then the resistance value begins to decay.

The reduction of the compressive strength for HAp-30 can be explained by the increase of porosity, associated with the greater amount of precipitate of salts in the preparation. The presence of different phases in the grain boundaries of a ceramic matrix of hydroxyapatite, mainly precipitates of salts, associated to the high porosity, contribute significantly to decrease the mechanical properties of the composite. The porosity and the presence of calcium aluminates in composite biomaterials make the grain boundaries weaker, contributing to a predominantly intergranular fracture mode. This can be noticed in micrographs represented by Fig. 4. According to Hannora [34], the mechanical properties are controlled not only by the amount of alumina addition but also by the heat treatment conditions. The improvement of mechanical strength with addition of alumina up to 15% may be due to the subsequent and partial transformation of HAp/Al_2O_3 into calcium aluminate, $CaAl_2O_4$. On the other hand, alumina in excess may result in reduced mechanical properties.

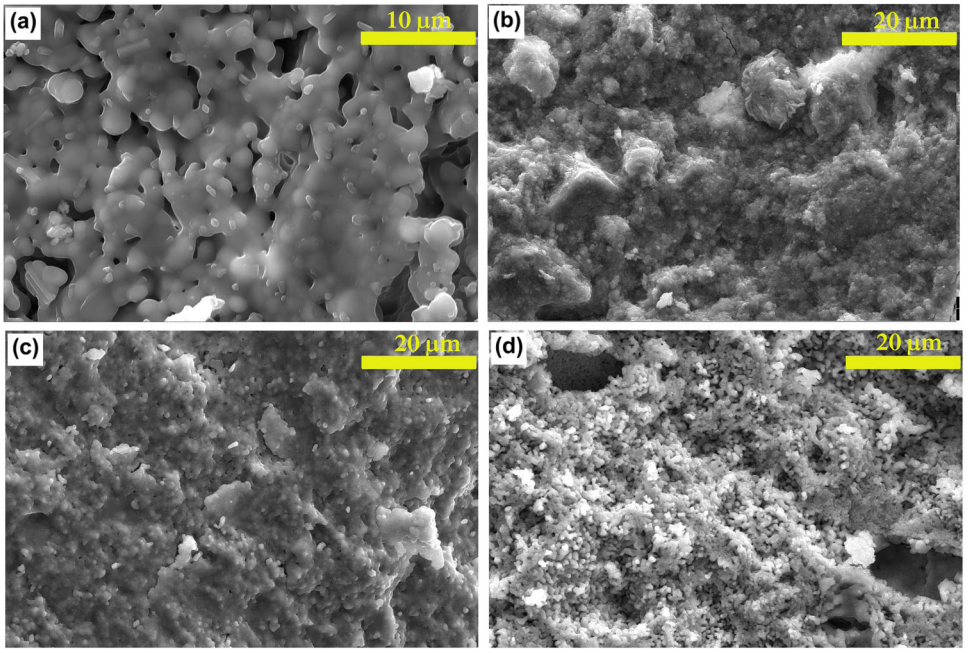

Fig. 4 SEM images of **a** HAp-00, **b** HAp-05, **c** HAp-15, and **d** HAp-30

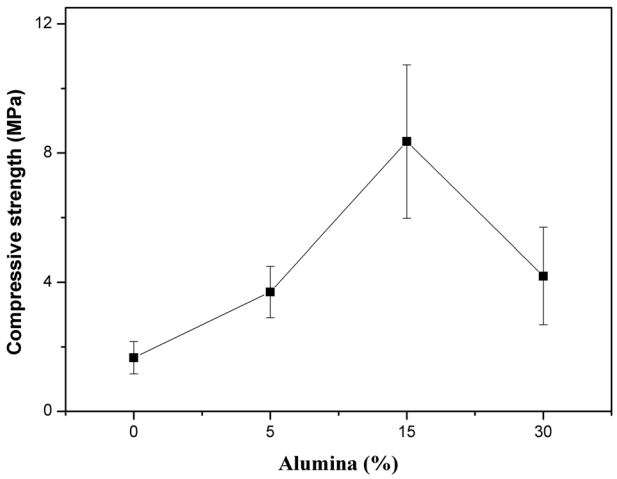

Fig. 5 Variation of compressive strength as a function of alumina addition

Table 3 Means and standard deviation of the diametral compression resistance

Treatments (%)	Mean resistance (MPa)	Standard deviation
0	1.66000	0.50120
5	3.69997	0.79501
15	8.35333	2.37692
30	4.18667	1.50434

Diametral compression results were subjected to ANOVA (Table 4) with significance level α of 0.05 in order to statistically verify if the arithmetic means of the resistances were not the same. It was observed that the additive had a significant influence on the mechanical properties of the composites at a confidence level of 95%. In this case, since the *p*-value (Prob > *F*) is less than the specified α of 0.05, null hypothesis (e.g., the means of all levels are equal) is rejected. Therefore, the means of one or more levels of diametral compression resistances are different.

Table 4 Analysis of variance of diametral compression strength at four levels

Source of variation	Sum of squares	Degree of freedom	Mean square	*F* value	Prob>*F*
Additive	70.96389	3	23.65463	10.75699	0.00351
Residue	17.592	8	2.199		
Total	88.55589	11			

Table 5 Results of Tukey–Kramer test of diametral compression strength

Comparison levels	Absolute difference	Standard error of difference	*q* Value	Sig
5–0	2.03667	1.21078	2.37885	0
15–0	6.69333	1.21078	7.81791	1
15–5	4.65667	1.21078	5.43905	1

As the test showed differences between levels, Tukey's multiple comparisons method (Table 5) was used to determine which levels show statistically significant differences. Two means are considered significantly different by the Tukey–Kramer criterion if the absolute difference in the arithmetic means of the samples is greater than a critical range.

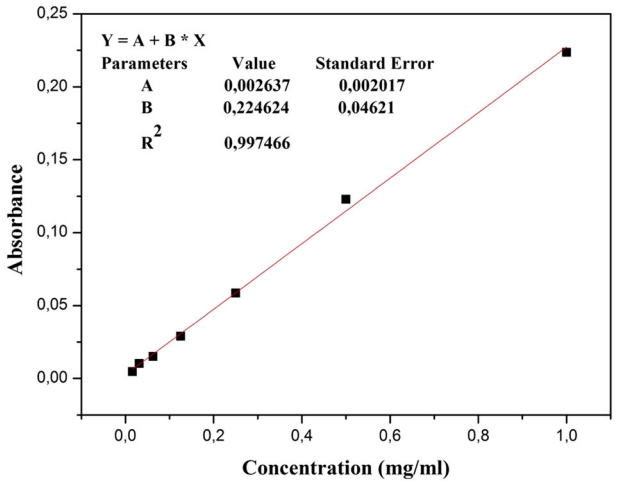

Fig. 6 Standard calibration curve for ampicillin by UV absorption spectrophotometry

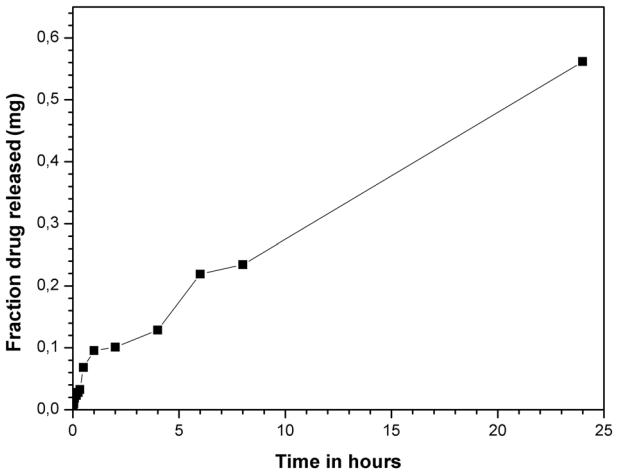

Fig. 7 Antibiotic release profile of HApF-15 as a function of the immersion time in PBS

Sig equals 1 indicates that the means difference is significant at the 0.05 level. Sig equals 0 indicates that the mean difference is not significant at the 0.05 level. The data indicate that there are significant differences between the levels 15–0 and 15–5 but not between 5 and 0. This implies that 0 and 5% of alumina concentration produces approximately the same resistance to diametral compression and that all other levels possess different resistances. Therefore, it is possible to conclude, at a confidence level of 95%, that the HAp-05 presents lower resistance to diametral compression than the HAp-15.

3.6 Controlled release of antibiotic

Figure 6 shows the calibration curve obtained by UV-Vis spectrophotometry for ampicillin in buffer (PBS). The calibration curve was linear ($R^2 = 0.997466$) over a concentration range from 0.01 to 1.0 mg/ml.

In order to investigate the influence of the structural characteristics of the composite on the release of ampicillin, the HAp-15 was tested with the incorporation of 1% by weight of ampicillin. The percentage of antibiotic was calculated with regard to the mass of the solid phase (1.06 g). The drug release profile as a function of the time is presented in Fig. 7.

The results indicate that in 24 h of the experiment, 5.29% of the drug is released. Initially, the dissolution and immediate release of the drug located on the surface of the composite takes place. Subsequently, the decrease in release rate probably occurs as a function of the quantity of drug incorporated and the amount of pores present in the sample. The alumina incorporated into the composite reduces its apparent porosity and, due to geometric considerations, impairs the diffusion of the drug along the voids available in

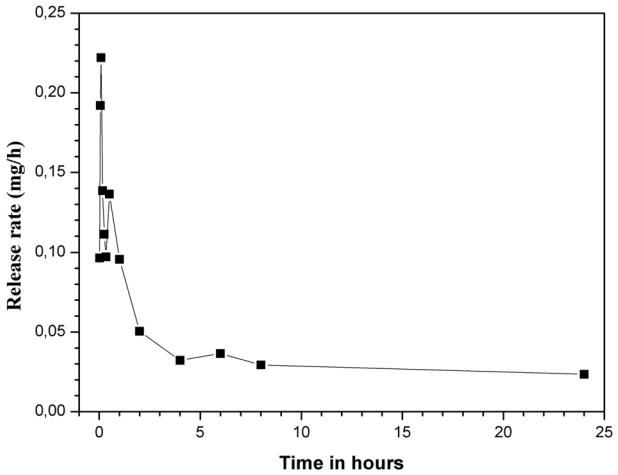

Fig. 8 Ampicillin release rate of composite HApF-15

the structure. The porosity of the matrix used and the amount of drug incorporated can also affect the release of biomaterial-based drugs. The porosity of the matrix in this case is formed by the initial intrinsic porosity of the material and by the porosity formed by the dissolution of the antibiotic.

The liberation rate of ampicillin in the HApF-15 is shown in Fig. 8. The composite exhibits an atypical release rate in the first 10 min and then assumes the expected profile, since the amount of drug released decreases with time. This variation is due to changes in the surface of the hydroxyapatite grains, as observed in the SEM images.

It is worth emphasizing that the slow release of drugs may not provide the desired therapeutic effect and even provoke resistance of the bacterium to the antibiotic. In this regard, there are several factors that influence the release of

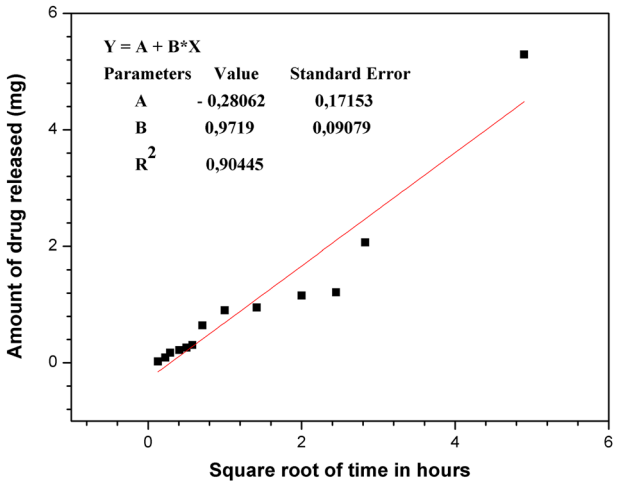

Fig. 9 Higuchi model for the study of ampicillin release from HApF-15

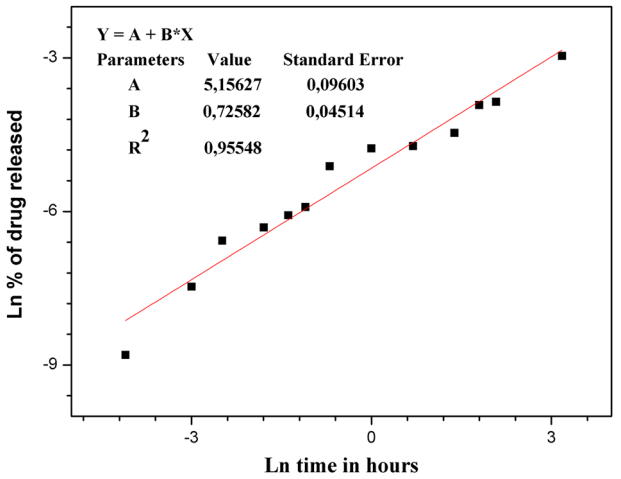

Fig. 10 Korsmeyer–Peppas model for ampicillin release from HApF-15

the drug [22], such as the structure, the type of interaction between the drug and the matrix, and the mechanism of degradation of calcium phosphate.

Several mathematical models have been published, to elucidate drug transport processes and to predict the resulting drug release kinetics. However, the mathematical description of the entire drug release process is rather difficult, because of the number of physical characteristics that must be taken into consideration [35]. Each model makes certain assumptions and due to these assumptions, the applicability of the respective models is restricted to certain drug–polymer systems [35].

Higuchi model can be used to describe the dissolution of drugs from various pharmaceutical modified-release forms [36]. Considering the linear trend-line of this test, Fig. 9 shows that the amount of ampicillin released as a function of the square root of time obeys the Higuchi model in the first 2 h of release. During this time, release of the drug from the HApF-15 is controlled by a diffusion process in the pores, indicating that the release depends on the porosity of the matrix [37].

The Korsmeyer–Peppas model is generally used to analyze the release from calcium phosphate matrix when the release mechanism is non-Fickian [38]. Following this mathematical model, release of ampicillin from the composite was represented by linear behavior (Fig. 10). The linear regression showed a release exponent value $n = 0.96$. Then, ampicillin is released due to an anomalous transport not governed by Fick diffusion [36, 39].

The anomalous release behavior occurs when the rates of diffusion and relaxation are of the same order of magnitude. In other words, release is associated not only with drug diffusion but also with conformational changes of the polymer. Factors such as change in crystallinity and reduction of the amount of drug within the matrix can lead to an anomalous diffusion [36].

4 Conclusions

The increase of the amount of alumina in the composites favors the degradation of HAp during the sintering, with formation of tricalcium phosphate and calcium aluminates.

In this paper, the release study of ampicillin with HAp-15 showed a rapid release in the first hour, following the Higuchi model. This type of release can prevent a very low concentration of the drug at the beginning of treatment of an infection, thereby avoiding an ineffective therapeutic effect and even possible bacterial resistance to the antibiotic.

Analysis of the release profile using the Korsmeyer–Peppas model showed that ampicillin is released from the composites by an anomalous transport process not governed by Fick diffusion. This behavior may be desirable if it allows such release devices to be employed in different clinical applications which require distinct treatment times.

In general, the hydroxyapatite synthesized by sol–gel technique, as described in this article proved to be suitable for the preparation of hydroxyapatite-based composites (HAp–Al_2O_3) with potential to produce devices for use in drug delivery systems.

Acknowledgements We are thankful to Fundação Cearense de Apoio ao Desenvolvimento Científico e Tecnológico (FUNCAP, Brazil) for their financial support.

Compliance with ethical standards

Conflict of interest The authors declare that they have no competing interests.

References

1. Coelho J, Ferreira P, Alves P, Cordeiro R, Fonseca A, Góis J, et al. (2010) Drug delivery systems: advanced technologies potentially applicable in personalized treatments 1:164–209
2. Kleiner LW, Wright JC, Wang Y (2014) Evolution of implantable and insertable drug delivery systems. J Control Release 181:1–10
3. Mitra S, Maitra A (2009) Inorganic Nanoparticles for Therapeutics, Drug and Gene Delivery. C.E.N.T.E.R.A., in book: Advances in Nanotechnology and Applications (vol. 1)
4. Cicuendez M, Izquierdo-Barba I, Portoles MT, Vallet-Regi M (2013) Biocompatibility and levofloxacin delivery of mesoporous materials. Eur J Pharm Biopharm 84:115–124
5. Guo YJ, Wang YY, Chen T, Wei YT, Chu LF, Guo YP (2013) Hollow carbonated hydroxyapatite microspheres with mesoporous structure: hydrothermal fabrication and drug delivery property. Mater Sci Eng C Mater Biol Appl 33:3166–3172
6. Wertheimer AI, Santella TM, Finestone AJ, Levy RA (2005) Drug delivery systems improve pharmaceutical profile and facilitate medication adherence. Adv Ther 22:559–577
7. Farzadi A, Solati-Hashjin M, Bakhshi F, Aminian A (2011) Synthesis and characterization of hydroxyapatite/β-tricalcium phosphate nanocomposites using microwave irradiation. Ceram Int 37:65–71
8. Ravarian R, Moztarzadeh F, Hashjin MS, Rabiee SM, Khoshakhlagh P, Tahriri M (2010) Synthesis, characterization and bioactivity investigation of bioglass/hydroxyapatite composite. Ceram Int 36:291–297
9. Duarte EB, Chagas BS, Andrade FK, Brígida AIS, Borges MF, Muniz CR et al. (2015) Production of hydroxyapatite–bacterial cellulose nanocomposites from agroindustrial wastes. Cellulose 22:3177–3187
10. Reis ECC, Borges APB, Fonseca CC, Martinez MMM, Eleotério RB, Morato GO et al. (2010) Biocompatibility, osteointegration, osteoconduction, and biodegradation of a hydroxyapatite-polyhydroxybutyrate composite. Braz Arch Biol Technol 53:817–826
11. Kumta PN, Sfeir C, Lee D-H, Olton D, Choi D (2005) Nanostructured calcium phosphates for biomedical applications: novel synthesis and characterization. Acta Biomater 1:65–83
12. Liu D-M, Troczynski T, Tseng WJ (2001) Water-based sol–gel synthesis of hydroxyapatite: process development. Biomaterials 22:1721–1730
13. Horng Yih J, Min Hsiung H (1994) Fabrication and mechanical properties of hydroxyapatite-alumina composites. Mater Sci Eng C 2:77–81
14. Raj SV, Rajkumar M, Sundaram NM, Kandaswamy A (2018) Synthesis and characterization of hydroxyapatite/alumina ceramic nanocomposites for biomedical applications. Bull Mater Sci 41:93
15. Gautier S, Champion E, Bernache-Assollant D (1999) Toughening characterization in alumina platelet-hydroxyapatite matrix composites. J Mater Sci Mater Med 10:533–540
16. Yelten A, Yilmaz S, Oktar FN (2012) Sol–gel derived alumina–hydroxyapatite–tricalcium phosphate porous composite powders. Ceram Int 38:2659–2665
17. Viswanath B, Ravishankar N (2006) Interfacial reactions in hydroxyapatite/alumina nanocomposites. Scr Mater 55:863–866
18. Landi E, Tampieri A, Celotti G, Sprio S (2000) Densification behaviour and mechanisms of synthetic hydroxyapatites. J Eur Ceram Soc 20:2377–2387
19. Driscoll WC (1996) Robustness of the ANOVA and Tukey-Kramer statistical tests. Comput Ind Eng 31:265–268
20. Higuchi T (1961) Rate of release of medicaments from ointment bases containing drugs in suspension. J Pharm Sci 50:874–875
21. Korsmeyer R, Peppas N (1983) Macromolecular and modeling aspects of swelling-controlled systems. Control Release Deliv Syst 1983:77–90
22. Wang S Ordered mesoporous materials for drug delivery (2009) 117:1–9
23. Hsieh MF, Perng LH, Chin TS, Perng HG (2001) Phase purity of sol-gel-derived hydroxyapatite ceramic. Biomaterials 22:2601–2607
24. Best SM, Porter AE, Thian ES, Huang J (2008) Bioceramics: past, present and for the future. J Eur Ceram Soc 28:1319–1327
25. Santos MH, Oliveira Md, LPdF Souza, Mansur HS, Vasconcelos WL (2004) Synthesis control and characterization of hydroxyapatite prepared by wet precipitation process. Mater Res 7:625–630
26. Manoj M, Subbiah R, Mangalaraj D, Ponpandian N, Viswanathan C, Park K (2015) Influence of growth parameters on the formation of hydroxyapatite (HAp) nanostructures and their cell viability studies. Nanobiomedicine 2:2
27. Ji H, Marquis PM (1993) Sintering behaviour of hydroxyapatite reinforced with 20 wt % Al2O3. J Mater Sci 28:1941–1945
28. Evis Z, Doremus RH (2007) A study of phase stability and mechanical properties of hydroxylapatite–nanosize α-alumina composites 27:421–425
29. Jun YK, Kim WH, Kweon OK, Hong SH (2003) The fabrication and biochemical evaluation of alumina reinforced calcium phosphate porous implants. Biomaterials 24:3731–3739
30. Tampieri A, Celotti G, Sprio S, Mingazzini C (2000) Characteristics of synthetic hydroxyapatites and attempts to improve their thermal stability 54–61
31. Mezahi F-Z, Oudadesse H, Harabi A, Le Gal Y (2012) Effect of ZrO2, TiO2, and Al2O3 additions on process and kinetics of bonelike apatite formation on sintered natural hydroxyapatite surfaceS. Int J Appl Ceram Technol 9:529–540
32. Epure LM, Dimitrievska S, Merhi Y, Yahia L (2007) The effect of varying Al2O3 percentage in hydroxyapatite/Al2O3 composite materials: morphological, chemical and cytotoxic evaluation. J Biomed Mater Res A 83:1009–1023
33. Bartonickova E, Vojtisek J, Tkacz J, Pořízka J, Masilko J, Moncekova M, et al (2017) Porous HA/Alumina composites intended for bone-tissue engineering 51:631–636
34. Hannora A (2014) Preparation and characterization of hydroxyapatite/alumina nanocomposites by high-energy vibratory ball milling 293–307
35. Shoaib MH, Tazeen J, Merchant HA, Yousuf RI (2006) Evaluation of drug release kinetics from ibuprofen matrix tablets using HPMC. Pak J Pharm Sci 19:119–124
36. Costa P, Sousa Lobo JM (2001) Modeling and comparison of dissolution profiles. Eur J Pharm Sci 13:123–133
37. Martins VC, Goissis G, Ribeiro AC, Marcantonio Jr. E, Bet MR (1998) The controlled release of antibiotic by hydroxyapatite: anionic collagen composites. Artif Organs 22:215–221
38. Ginebra M-P, Canal C, Espanol M, Pastorino D, Montufar EB (2012) Calcium phosphate cements as drug delivery materials. Adv Drug Deliv Rev 64:1090–1110
39. Peppas NA (1985) Analysis of Fickian and non-Fickian drug release from polymers. Pharm Acta Helv 60:110–111